

# Low Cost High-Speed Test Data Acquisition: Accurate Period Estimation Driven Signal Reconstruction Using Incoherent Subsampling

Thomas Moon, Hyun Woo Choi, Abhijit Chatterjee  
School of ECE, Georgia Tech, USA

**Abstract**—In this paper, we propose a new algorithm to estimate the fundamental period (frequency) of a high-speed pseudo random bit sequence (PRBS) or multitone signal using incoherent subsampling. While incoherent subsampling suffers from spectral leakage due to the mismatch between the input test signal and the discrete Fourier transform (DFT) basis, the proposed algorithm efficiently resolves the spectral leakage problem using a back-end signal process. The approach requires incoherent digitization of the periodic sequence using at least two clocks running at different speeds. No additional hardware to synchronize the input signal frequency with the sampling clock frequency is needed. A new discrete frequency shifting approach for determining the period of the input signal is proposed that is computationally efficient. The signal reconstruction approach has been tested with experimental results.

## I. INTRODUCTION

THE Whittaker, Kotelnikov and Shannon (WKS) theorem is the most fundamental theory says that a signal band-limited to  $H$  Hertz can be recovered with  $2H$  samples per second [1]. When a signal is subsampled, the spectrum of the signal is aliased allowing less information about the signal to be recovered in general. Further, while subsampling, it is difficult to sample coherently as this requires precise knowledge of the period of the signal being subsampled. In specific test applications, it is possible to know the range of values possible for the period of the test signal but not the exact period value. In other cases, it is simply difficult to synchronize the test signal with the sampling clock signal unless specific high-speed signal synchronization mechanisms are used. Unlike coherent sampling, incoherent sampling suffers from spectral leakage which causes difficulty in analyzing the spectrum of a digitized signal. To resolve this problem, a number of research has been investigated with compressive sampling (CS). Replacing the DFT basis with a redundant frame of sinusoids which is called a DFT frame is used to increase the resolution of the standard DFT and reduce the mismatch between the

input test signal and the DFT basis [2], [3].

In [4], a high-speed periodic signal acquisition technique using incoherent subsampling is presented. They estimate the discrete frequency of the digitized signal using a DFT spectrum based on Gaussian interpolation [5]. Using the knowledge of the estimated fundamental discrete frequency, the signal is reconstructed in the time-domain. The accuracy to which the discrete frequency is estimated directly determines the noise in the reconstructed time-domain signal. The jitter in the time-domain signal representation is then suppressed using back-end signal processing algorithms.

This paper focuses on accurate estimation of the discrete frequency of a periodic signal and proposes a new method which achieves better accuracy than Gaussian interpolation. As mentioned earlier, this is critical for reducing the noise in the time-domain reconstructed signal. The computation time of the proposed method is not aggressive because it is based on the Fast Fourier Transform (FFT). Furthermore, our algorithm can be applied to construct eye diagrams of pseudo random bit sequences (PRBSs) without any hardware such as clock data recovery (CDR) circuit. The proposed method is expected to achieve better performance in jitter characterization in the future.

To summarize, the following are key benefits of this research:

- It is possible, using our algorithm, to accurately estimate the period (frequency) of a high-speed periodic input test signal including PRBSs using incoherent subsampling.
- The proposed algorithm does not require additional hardware to synchronize the input signal frequency with the sampling clock frequency.
- By our algorithm, eye diagrams of PRBSs can be constructed without CDR circuit.

In Section II, we describe the proposed method and the related theory of discrete frequency estimation along with the results of computer simulations. Hardware ex-

periment results are summarized in Section III. Finally conclusions are presented.

## II. PROPOSED METHOD

In general, coherent sampling is a preferred way to receive analog signal and perform the DFT of the acquired discrete samples, which is the most common tool in signal spectral analysis [6], [7]. In coherent sampling, a periodic signal is sampled over an integer number of its periods to avoid unwanted discontinuities in the signal, and guarantees that the power spectrum of the fundamental frequency component is located exactly at the DFT frequency bin. Thus, coherent sampling minimizes the DFT spectral leakage of the measured signal. However, additional hardware to synchronize the input signal frequency with the sampling clock frequency is required to achieve this sampling coherency. A key requirement is that the fundamental frequency of the test signal to be measured should be known a priori.

On the other hand, incoherent sampling does not require the use of additional hardware for frequency/phase synchronization of the input signal and the sampling clock, and is used when the period of the input signal is not known or when such synchronization is difficult to achieve. However, incoherent sampling suffers from the spectral leakage across the DFT frequency bins. In the case of a PRBS or a multi-tone input signal, it is difficult to analyze the resulting complicated spectral components due to the spectral leakage. Moreover, the use of subsampling causes deterioration of the signal spectrum due to spectral folding/aliasing. The incoherent undersampling method proposed in this paper solves the spectral leakage problem and allows very accurate estimation of the fundamental period of the input signal enabling time-domain signal reconstruction with very high signal-to-noise ratio (SNR).

### A. Overview

The proposed method estimates the fundamental frequency of PRBS signals using incoherent subsampling with very fine resolution and only requires prior knowledge of the approximate range of the fundamental frequency (period) of the signal. Since this method only exploits the discrete data sampled from the input signal, it can be implemented by a simple hardware setup such as a single ADC and a programmable PLL or an adjustable external clock generator for sampling clock. Fig. 1 shows the overall flow chart of the proposed method which is composed of three steps: 1) coarse estimation of discrete fundamental frequency( $f_d$ ) by multirate subsampling, 2) fine estimation of  $f_d$  by discrete frequency shifting and

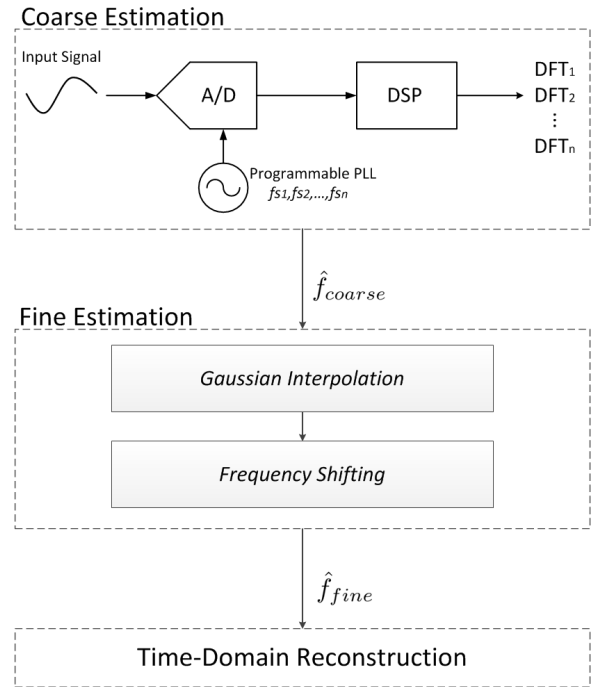


Fig. 1. Overview of the proposed method for accurate estimation of a discrete fundamental frequency value and the time-domain reconstruction.

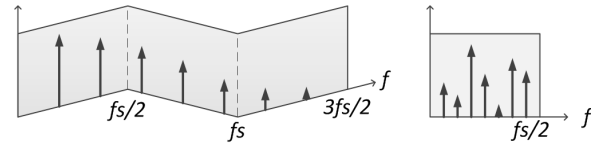


Fig. 2. Subsampling the original spectrum effectively folds the frequency domain by  $f_s/2$  and results in aliasing tones.

3) signal reconstruction in the time-domain based on the estimated  $f_d$ . In coarse estimation of  $f_d$ , we compare the discrete Fourier transform (DFT) spectra sampled at two different sampling rates. The coarse  $f_d$  can be estimated from analysis of the spectrum and knowledge of the sampling rate. Then, the fine  $f_d$  is estimated with much higher resolution by using a new “discrete frequency shifting” algorithm. Finally, the input signal is reconstructed in the time-domain based on the estimated discrete fundamental frequency.

### B. Coarse Estimation of Discrete Fundamental Frequency: Multirate Subsampling

Multirate subsampling is used to estimate the coarse discrete fundamental frequency. As shown in Fig. 2., the original spectrum of the signal is “scrambled” due to frequency aliasing effect resulting from digital subsampling. Subsampling can be thought as folding the frequency domain by the half of sampling rate,  $f_s/2$ , referred to as the Nyquist zone [8]. Note that the resulting

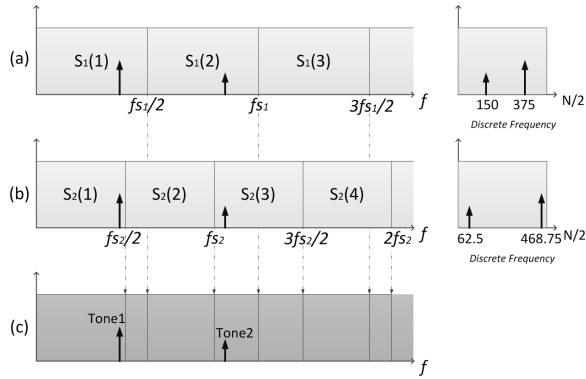


Fig. 3. Examples of multirate sampling rates. Different discrete spectra are achieved in the discrete frequency domain from the same original test signal.

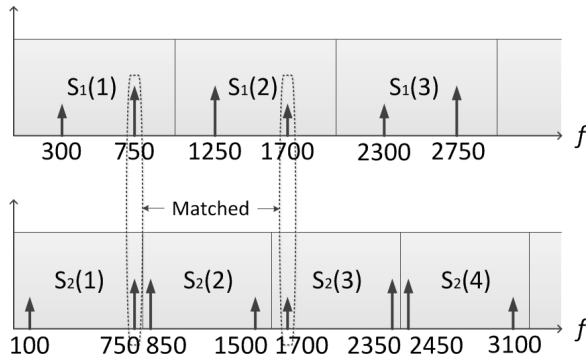


Fig. 4. Spreading DFT spectra by multirate and converting to analog frequency. In this example, two tones at 750MHz and 1700MHz are matched.

aliased spectrum is dependent on the sampling rate  $f_s$ .

Let  $f_{s1}$  and  $f_{s2}$  be two different sampling rates where  $f_{s1} > f_{s2}$ . Then, for the same analog test signal, two different sampling rates generate two different DFT spectra as shown in Fig. 3. Since the subsampled DFT spectrum presents in the folded frequency domain, “unfolding back” the folded spectrum generates the possible spectrum candidates for the original (unfolded, Nyquist rate) spectrum. Fig. 4 shows the “unfolding back” DFT spectra from the subsampled signals for different sampling rates. Before describing the proposed unscrambling method in detail, let us first consider a simple and intuitive example.

*Example:* We will first illustrate how the analog frequency of the signal converts into the discrete frequency. Let a signal have two tones at  $f_{t1} = 750\text{MHz}$  (T1) and  $f_{t2} = 1.7\text{GHz}$  (T2) as shown in Fig. 3(c). The signal is sampled at two different sampling rates,  $f_{s1} = 2\text{GHz}$  and  $f_{s2} = 1.6\text{GHz}$ , and the number of obtained discrete samples is  $N = 1000$  for both. For the first sampling rate ( $f_{s1} = 2\text{GHz}$ ), T1 and T2 are located in the first and the second Nyquist zone, respectively. Note that T2 is

aliased. The discrete frequency of the two tones are

$$D_{t1,s1} = |750 - 0| \cdot \frac{1000}{2000} = 375$$

$$D_{t2,s1} = |1700 - 2000| \cdot \frac{1000}{2000} = 150$$

Similarly, for the second sampling rate ( $f_{s2} = 1.6\text{GHz}$ ), T1 and T2 are located in the first and the third Nyquist zone, respectively. The discrete frequency of the two tones are

$$D_{t1,s2} = |750 - 0| \cdot \frac{1000}{1600} = 468.75$$

$$D_{t2,s2} = |1700 - 1600| \cdot \frac{1000}{1600} = 62.5$$

Note that the discrete frequency above is not normalized to  $2\pi$ .

Now, assume the measurement in reality. We may not know the analog frequency of the signal. In other words, the tones in the discrete spectrum could have been aliased or not. The core idea here is that list all the possible analog frequencies based on the two discrete spectra sampled at two different clock rates and find the common frequencies. The two DFT spectra are converted and unfolded in the analog frequency domain as shown in Fig. 4.  $S_1(n)$  and  $S_2(n)$  denotes the  $n$ -th Nyquist zone of the first and the second sampling rate, respectively. For example, the possible analog frequencies of  $D_{t2,s1}$  is obtained by

$$\left. \begin{aligned} \frac{2000}{1000} \cdot 150 &= 300\text{MHz} \\ \frac{2000}{1000} \cdot 150 + 2000 &= 2300\text{MHz} \dots \end{aligned} \right\} \text{odd Nyquist zone}$$

$$\left. \begin{aligned} 2000 - \frac{2000}{1000} \cdot 150 &= 1700\text{MHz} \\ 4000 - \frac{2000}{1000} \cdot 150 &= 3700\text{MHz} \dots \end{aligned} \right\} \text{even Nyquist zone}$$

In similar way, we can list the possible analog frequencies of  $D_{t2,s1}$ ,  $D_{t1,s2}$ ,  $D_{t2,s2}$  plotted in Fig. 4. The tones around 750MHz and 1700MHz are matched, indicating the frequencies of the two tones in the test input signal. These tones are referred to as “matched frequencies”.  $\square$

We now generalize the example. Let  $\hat{p}(i)$  and  $\hat{q}(i)$  be the discrete frequency of the  $i$ -th tone in the DFT sampled at  $f_{s1}$  and  $f_{s2}$ , respectively. Note that  $\hat{p}(i)$  and  $\hat{q}(i)$  are positive integers in  $[0, \frac{N}{2}]$  where  $N$  is the number of samples of the DFTs. Then, we can define unfolding the discrete frequencies,  $\hat{p}(i)$  and  $\hat{q}(i)$ , to

analog frequency domain as follows:

$$P_{odd}(i) = \{p|p = f_{s1}(k-1) + \frac{f_{s1}}{N}\hat{p}(i), k = 1, 2 \dots\} \quad (1)$$

$$P_{even}(i) = \{p|p = f_{s1}k - \frac{f_{s1}}{N}\hat{p}(i), k = 1, 2 \dots\} \quad (2)$$

$$P(i) = P_{odd}(i) \cup P_{even}(i) \quad (3)$$

$$Q_{odd}(i) = \{q|q = f_{s2}(k-1) + \frac{f_{s2}}{N}\hat{q}(i), k = 1, 2 \dots\} \quad (4)$$

$$Q_{even}(i) = \{q|q = f_{s2}k - \frac{f_{s2}}{N}\hat{q}(i), k = 1, 2 \dots\} \quad (5)$$

$$Q(i) = Q_{odd}(i) \cup Q_{even}(i) \quad (6)$$

where  $P_{odd}(i)$  and  $P_{even}(i)$  denote the set of the analog frequencies unfolded from the  $i$ -th discrete tone sampled at  $f_{s1}$  to the odd Nyquist zone and the even Nyquist zone, respectively. Likewise,  $Q_{odd}(i)$  and  $Q_{even}(i)$  denote the set of the analog frequencies unfolded from the  $i$ -th discrete tone sampled at  $f_{s2}$  to the odd Nyquist zone and the even Nyquist zone, respectively. The total unfolded spectra combining the odd and the even Nyquist components at  $f_{s1}$  and  $f_{s2}$  are denoted by  $P(i)$  and  $Q(i)$ , respectively. Fig. 4 illustrates the unfolded spectrum.

Note that the tones might not be exactly matched at the same frequency as in Fig. 4 because the spectral leakage across the DFT frequency bins cause errors in the conversion to analog frequency from digital frequency. Even though the resolution of the estimation is not very fine, we can see that the coarse frequency of the tones can be determined by comparing the unfolded DFT spectrum from different sampling rates and seeing if common frequency points exist in the related spectra. However, it is not guaranteed that the matched frequencies will always be the correct frequencies of the input tones. For example, if we look further into higher frequencies, other frequencies are matched at 6300MHz, 7250MHz, and so on. To reduce the unwanted matched-frequencies, another sample set at a different sampling rate is added,  $f_{s3} = 1.8\text{GHz}$  for this example. Then, the lowest unwanted matched-frequency becomes 14.3GHz. In practice, since the input test signal is bandlimited, there exists an upper frequency bound which excludes unreasonable matched frequencies. This criterion is used to limit the search for matched frequencies originating from frequency “unfolding”.

When the input signal is a PRBS signal, its fundamental frequency is more likely to be located near the low end of the frequency spectrum. This is because the fundamental frequency of a PRBS with a bit period of  $l$  and a bit rate of  $f_b$  is  $l/f_b$  and the rest of tones are simply harmonics of the fundamental tone [9]. In other words, a longer-bit-period-PRBS has a lower fundamental frequency. For this reason, it is

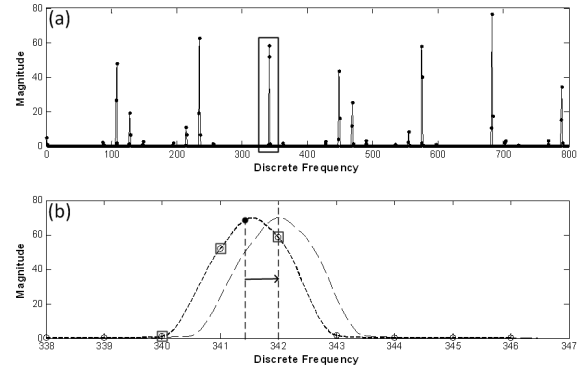


Fig. 5. (a) DFT spectrum of the simulated PRBS signal.  $\hat{f}_{coarse}$  is indicated by the black box. (b) The spectrum near  $\hat{f}_{coarse}$  is zoomed-in.  $\hat{f}_{Gauss}$  (denoted by the black dot) is estimated by three spectral points (denoted by squares). The initial shift is operated.

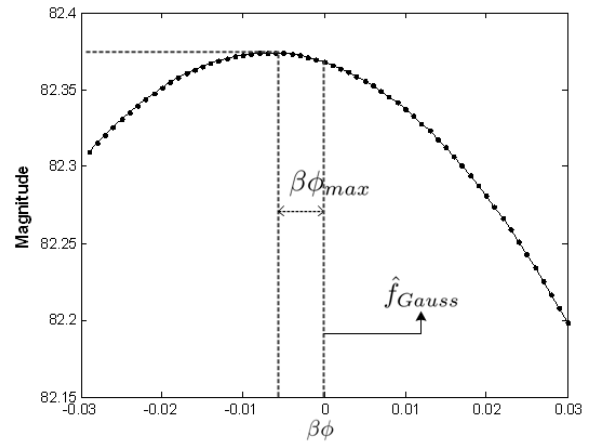


Fig. 6. Fine resolution shift over the sweeping range: The magnitude of shifted DFT spectrum at the target DFT is plotted over the amount of shifting. Starting from  $\hat{f}_{Gauss}$ , the DFT spectrum is shifted to left and right. Denote  $\phi_{max}$  when the maximum is achieved.

sufficient to unfold the discrete DFT spectrum to just a few orders of the Nyquist zone. Thus, the integer  $k$  described in (1),(2),(4), and (5) can be a finite number. Once the frequency location of the PRBS spectrum near the baseband are determined, we can find the lowest frequency value among several matched-frequencies to locate the fundamental frequency. We denote this coarse fundamental frequency  $\hat{f}_{coarse}$  which can be described as

$$\hat{f}_{coarse} = \min \left( \left( \bigcup_{i=1}^{n_1} P(i) \right) \cap \left( \bigcup_{i=1}^{n_2} Q(i) \right) \right)$$

where the number of tones detected in the DFT sampled at  $f_{s1}$  and  $f_{s2}$  is  $n_1$  and  $n_2$ , respectively.

### C. Fine Estimation of Discrete Fundamental Frequency: Discrete Frequency Shifting

To reduce the spectral leakage and enhance the resolution of the DFT spectrum, [4] introduce the combination of windowing and interpolation. Multiplying a window function (Gaussian, Hamming, etc) with the sampled signal, the windowed DFT spectrum achieves less spectral leakage. To enhance the spectrum resolution for locating the spectral peak, the spectral points are interpolated by Gaussian interpolation [5]. Based on the coarse discrete fundamental frequency  $\hat{f}_{coarse}$  in section 2.2, the three spectral points (marked as squares in Fig. 5(b)) near  $\hat{f}_{coarse}$  (marked as the box in Fig. 5(a)) can be selected. Using the Gaussian interpolation formula,

$$\hat{f}_{Gauss} = l + \frac{\ln\left(\frac{X[l+1]}{X[l-1]}\right)}{2 \ln\left(\frac{X[l]^2}{X[l+1]X[l-1]}\right)}$$

where  $X[l-1]$ ,  $X[l]$ ,  $X[l+1]$  are the three spectral points, the discrete Gaussian interpolated fundamental frequency is achieved and denoted by  $\hat{f}_{Gauss}$  (marked as a black dot in Fig. 5(b)).

We introduce a new method to further enhance the spectral resolution from the Gaussian interpolation. The idea is “shifting” (or “modulation”) the discrete spectrum of incoherent sampling to fit into the DFT frequency bins. The discrete frequency of the fundamental tone which is not exactly located in a DFT bin suffers spectral leakage into the neighbor bins. Therefore, if the tone is slightly shifted close to the DFT bin, the magnitude of the DFT bin will increase. When the shifted tone is exactly located on the DFT bin, the magnitude of the bin will have a maximum. The magnitude of the bin will decrease as the shifted tone moves away from the bin. The DFT is defined as

$$X[k] = \sum_{n=1}^N x[n] e^{-j2\pi \frac{k}{N} n}$$

where  $x_1, \dots, x_N$  is the  $N$ -sampled signal. Then, the frequency shift in the DFT is easily done by the DFT property as following [10]:

$$e^{j2\pi nl/N} x[n] \xrightarrow{DFT} X[(k-l)_N] \quad (7)$$

where  $(n)_N$  denotes  $(n \text{ modulo } N)$ . However, as the frequency will be shifted less than a DFT bin size in our proposed method and usually our interested DFT bin is not on the edge of the DFT (0 or  $N$ ), we will simply use  $X[k-l]$  instead of  $X[(k-l)_N]$ .

Since  $\hat{f}_{Gauss}$  is a good estimator for the peak, we first use  $\hat{f}_{Gauss}$  as the initial step for the shift. Fig. 5(b) shows that the discrete spectrum is shifted to locate the peak of the tone estimated by Gaussian interpolation as

close to a DFT bin as possible. We define  $n_t$  to be the index of the target DFT bin where the peak is shifted. Once the peak is shifted to the target DFT bin of  $n_t$ , the discrete spectrum is shifted again with finer resolution. Since we do not know whether the true peak locates lower or higher than  $\hat{f}_{Gauss}$ , the shift is swept over a desired range centered at  $\hat{f}_{Gauss}$ .

The initial shift based on the Gaussian interpolation is described as

$$e^{j2\pi n \Delta f_{Gauss}/N} x[n] = x_g[n] \xrightarrow{DFT} X_g[k]$$

where  $x[n]$  are the length- $N$ -samples for  $n = 1, 2, \dots, N$ , and  $\Delta f_{Gauss} = \lceil \hat{f}_{Gauss} \rceil - \hat{f}_{Gauss}$ . Then, the fine shift swept over a desired range centered at  $\hat{f}_{Gauss}$  is described as

$$e^{j2\pi n \phi \beta / N} x_g[n] \xrightarrow{DFT} X_\phi[k]$$

where  $\beta < 1$  is the desired fine-step resolution, and  $\phi = -r, -r+1, \dots, r$  where  $r$  is the desired sweeping range. As the magnitude of the target DFT bin is changing over the sweep, we can find the maximum value of the magnitudes. We denote  $\phi_{max}$  as the sweeping offset when the target DFT bin has the maximum value and  $\phi_{max}$  can be expressed as

$$\phi_{max} = \arg(\max(|X_{-r}[n_t]|, |X_{-r+1}[n_t]|, \dots, |X_r[n_t]|))$$

Fig. 5 and Fig. 6 illustrate a particular case for the fine estimation of the fundamental frequency. In computer simulation, a 5.121-Gbps 15-bit PRBS was subsampled at 1.6-Gsps with 1596 samples. Hamming window was applied to reduce the spectral leakage. The coarse fundamental frequency near the 341st bin is obtained by the coarse estimation step. By Gaussian interpolation,  $\hat{f}_{Gauss}$  is calculated as 341.5309. We choose the 342nd bin for the target bin and the spectrum is shifted to the bin as shown in Fig. 5(b). In the fine estimation, we set the resolution  $\beta = 0.001$  and the sweeping range  $r = 60$ . During the spectrum-shifting, we can plot the magnitude of the target DFT bin over the sweep. Fig. 6 plots the relationship between the  $\beta\phi$  and the magnitude of the target DFT bin ( $X[342]$ ). The maximum magnitude of the target DFT bin corresponds when  $\phi$  is -7. In other words, if the spectrum is shifted to the leftward by 0.007 in discrete frequency, the true peak is located on the target DFT bin. This implies that the true peak is higher than  $\hat{f}_{Gauss}$  by 0.007 in discrete frequency. The fine discrete fundamental frequency,  $\hat{f}_{fine}$ , can be found by

$$\hat{f}_{fine} = \hat{f}_{Gauss} - \beta\phi_{max}$$

In the above example,  $\hat{f}_{fine}$  is calculated as 341.5374, whereas the true fundamental discrete frequency is 341.5465.

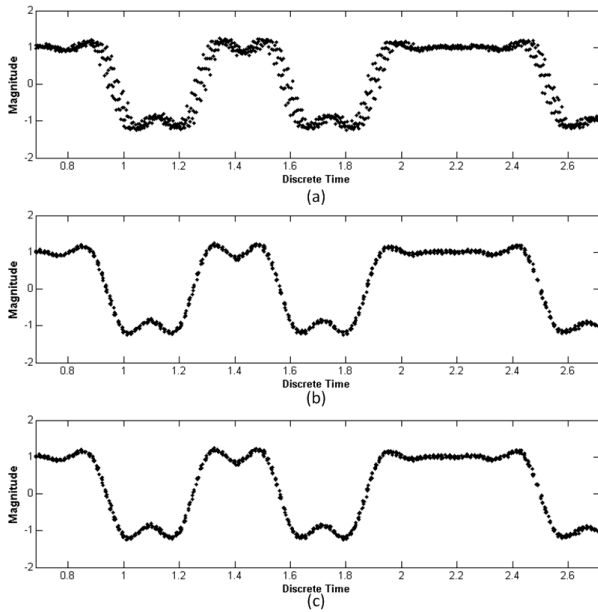


Fig. 7. Simulated signal reconstruction in the discrete time-domain based on (a) Gaussian interpolation, (b) proposed method, and (c) true fundamental frequency.

The amount of computation of the fine estimation is proportional to  $\beta\phi N$ . As the desired resolution and the sweeping range increases, the amount of computation increases. It is also obvious that the number of samples affects the amount of computation because the frequency shifting process involves the inner product of  $N$ -length vectors in (7). In future work, the amount of computation for finding  $\hat{f}_{fine}$  can be reduced by conjugate gradient method as the slope of Fig. 6 is smooth. Instead of sweeping the shifting frequency, calculating the instant slope for every step until the slope becomes close to 0 will reduce the computation time.

#### D. Signal Reconstruction in Time-Domain

In this section, the input signal is reconstructed in the time-domain based on the discrete fundamental frequency estimated by the proposed algorithm and Gaussian interpolation. The sampled signal  $x[n]$  is remapped to form the signal within the fundamental period. By the discrete-frequency-to-time-conversion introduced in [4], discrete time of a sampled signal is determined as

$$t_d[k] = \text{mod}(k, N/\hat{f}_d)$$

where  $\hat{f}_d$  is the estimated discrete fundamental frequency.

Fig. 7 compares the quality of the reconstructed signals by different estimations for the discrete fundamental frequency. We use the same simulation configuration in the previous section. Note that the reconstruction

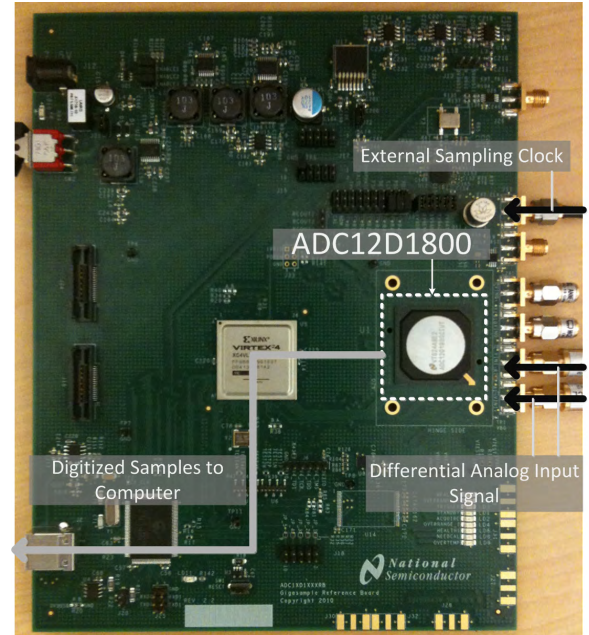


Fig. 8. Picture of experiment setup for the evaluation board of ADC12D1800.

TABLE I  
INPUT PRBS SIGNALS

PRBS	Bit period	Bit rate
A	31 bits	3.3GHz
B	63 bits	2.12GHz

quality depends on the accuracy of the estimated discrete fundamental frequency. Fig. 7(a) and (b) shows the reconstructed signals by Gaussian interpolation and our proposed method, respectively. Fig. 7(c) plots the reconstructed signal with the true discrete fundamental frequency calculated by the bit period and the bitrate of the input PRBS. As we can see in the plots, our proposed method can improve the quality of the time-domain reconstruction.

### III. HARDWARE EXPERIMENT

High-speed PRBS signals are generated by Agilent 81133A which supports 15MHz-3.35GHz frequency range with low jitter and generates PRBS bit period from  $2^5 - 1$  to  $2^{31} - 1$ . The PRBS signal is digitized by National Semiconductor ADC12D1800 evaluation board with 12-bit resolution and 1.8GHz maximum sampling clock in normal mode [11]. The experiment setup for the evaluation board is shown in Fig. 8. The digitized samples are collected by the internal FPGA of the evaluation board and transmitted to the computer. The external clock signal is provided by Agilent E4432B which supports 250MHz-3GHz sampling clock.

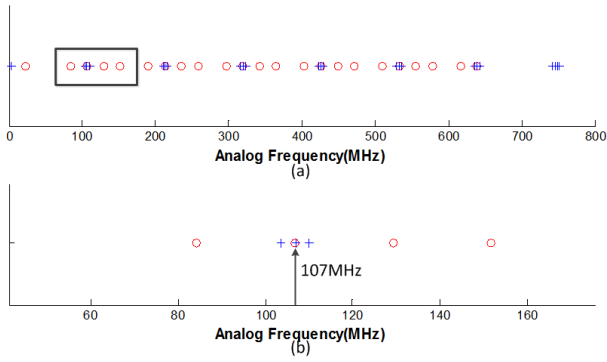


Fig. 9. The coarse estimation is performed for PRBS-A. (a) Red circles and blue circles denote the possible analog frequencies of the PRBS tones sampled at 1.6GHz and 1.3GHz, respectively. (b) the magnified view of the first matched tones(fundamental tone) around 107MHz.

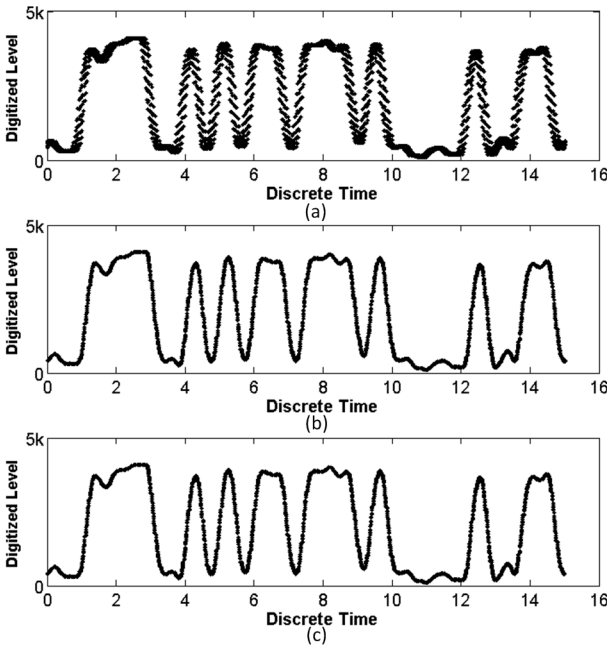


Fig. 10. PRBS-A reconstruction in the discrete time-domain based on (a) Gaussian interpolation ( $\hat{f}_{Gauss}$ ), (b) proposed method ( $\hat{f}_{fine}$ ), and (c) true fundamental frequency.

PRBSs signals are chosen for the test signal because the spectra of the PRBSs are usually more complicated than that of multi-tone signals. Since the original spectrum of a PRBS consists of an infinite number of harmonics of the fundamental tone, the subsampled discrete spectrum of the PRBS is difficult to unscramble. Therefore it is more challenging for PRBS signals to estimate the fundamental frequency using incoherent subsampling than for multi-tone signals. The bit period and the bit rate of the test PRBS signals for the hardware experiment is shown in Table I.

The input signals are sampled with two different sam-

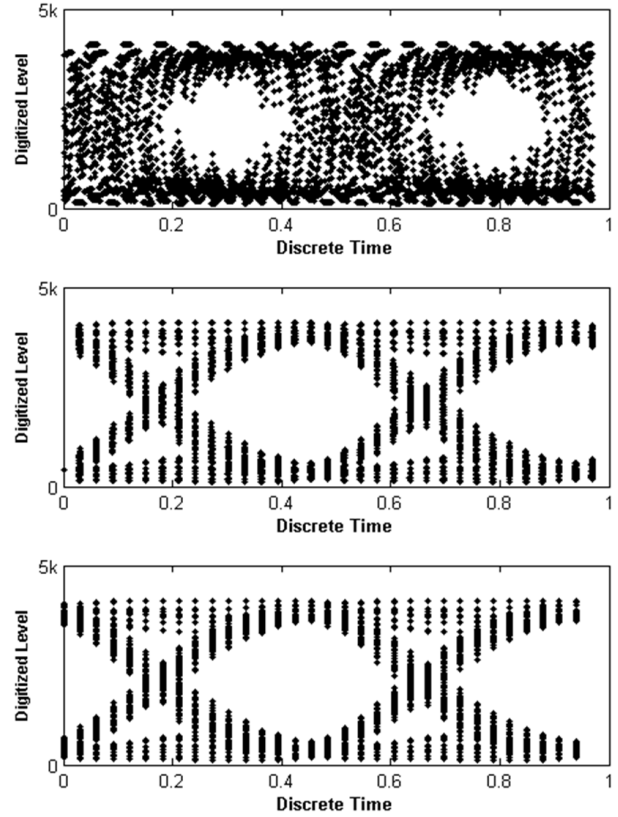


Fig. 11. The eye diagram of PRBS-A based on (a) Gaussian interpolation ( $\hat{f}_{Gauss}$ ), (b) proposed method ( $\hat{f}_{fine}$ ), and (c) true fundamental frequency.

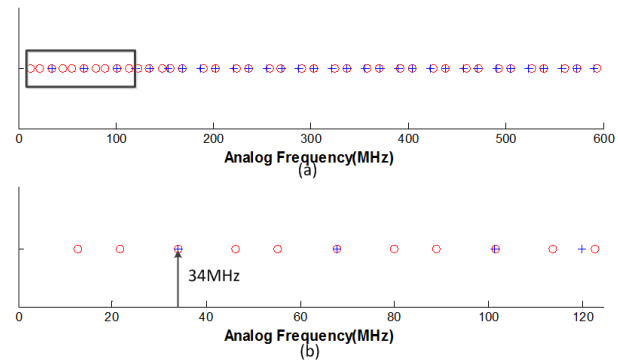


Fig. 12. The coarse estimation is performed for PRBS-B. (a) Red circles and blue circles denote the possible analog frequencies of the PRBS tones sampled at 1.6GHz and 1.3GHz, respectively. (b) the magnified view of the first matched tones(fundamental tone) around 34MHz.

pling clock rates, 1.6GHz and 1.3GHz. We collect 4096 samples from each sampling rate and apply the Hamming window to reduce the spectral leakage on the DFT spectrum. Fig. 9 shows the location of the tones in the unfolded DFT spectra of PRBS-A by the two sampling rates. It is observed that the first matched tone is around 107MHz, which corresponds to 276th bin of the 1.6GHz-



TABLE II  
SUMMARY OF THE RESULTS

	$\hat{f}_{coarse}$	$\hat{f}_{Gauss}$	$\hat{f}_{fine}$	$\hat{f}_{true}$	$e_{Gauss}$	$e_{fine}$
PRBS-A	276	275.629	275.645	275.6452	0.0162	0.0002
PRBS-B	88	87.805	87.822	87.8190	0.014	0.003

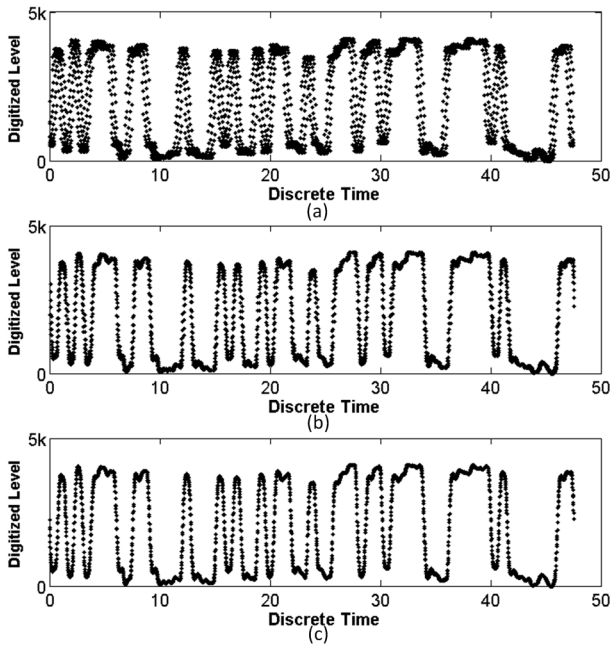


Fig. 13. PRBS-B reconstruction in the discrete time-domain based on (a) Gaussian interpolation ( $\hat{f}_{Gauss}$ ), (b) proposed method ( $\hat{f}_{fine}$ ), and (c) true fundamental frequency.

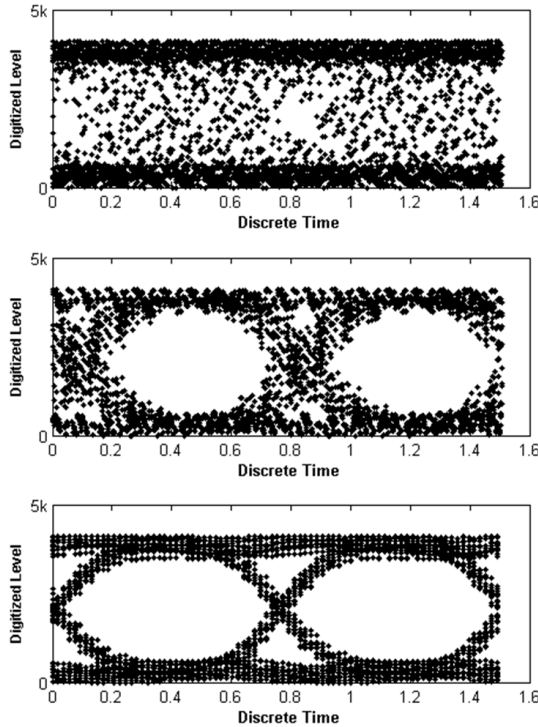


Fig. 14. The eye diagram of PRBS-B based on (a) Gaussian interpolation ( $\hat{f}_{Gauss}$ ), (b) proposed method ( $\hat{f}_{fine}$ ), and (c) true fundamental frequency.

sampling set ( $\hat{f}_{coarse} = 276$ ). Three spectral points are obtained centered at  $\hat{f}_{coarse}$ , and  $\hat{f}_{Gauss} = 275.629$  is achieved. Based on  $\hat{f}_{Gauss}$ ,  $\hat{f}_{fine} = 275.645$  is calculated with resolution  $\beta = 0.001$ . Fig. 10 compares the quality of the reconstructed signals by the different estimations for the discrete fundamental frequency. Based on the time-domain reconstructed signals, the eye diagrams are compared in Fig. 11.

In the case of PRBS-B signal, Fig. 12 shows the unfolded DFT spectra of PRBS-B by the two sampling rates, 1.6GHz and 1.3GHz. It is observed that the first matched tone is around 34MHz, which corresponds to 88th bin of the 1.6GHz-sampling set ( $\hat{f}_{coarse} = 88$ ). Three spectral points are obtained centered at  $\hat{f}_{coarse}$ , and  $\hat{f}_{Gauss} = 87.805$  is achieved. Based on  $\hat{f}_{Gauss}$ ,  $\hat{f}_{fine} = 87.822$  is calculated with resolution  $\beta = 0.001$ .

Table II summarizes the estimated discrete fundamental frequencies and the true discrete fundamental frequency based on the bit period and bit rate of the input PRBSs. Comparing the errors on the estimated discrete fundamental frequency, our proposed method achieves more accurate estimation which results in better performance in the time-domain reconstruction as shown in Fig. 10 and Fig. 13. Furthermore, the eye diagram of the test signals are shown in Fig. 11 and Fig. 14. It is clear that the eye opening of the proposed method is much larger than that of Gaussian interpolation.

#### IV. CONCLUSION

A new method to estimate the discrete fundamental frequency is proposed in this paper. Although the application of our algorithm is limited in the estimation of a periodic signal, the proposed method enhances the accuracy of the estimation and is compared with the existing method in the time-domain reconstruction. Since our algorithm is based on incoherent subsampling, no additional hardware for synchronization is required. Hardware measurement results are provided to support that the proposed method achieves better accuracy than Gaussian interpolation. Another benefit of the proposed method is efficiency of computation. In the fine estimation, shifting discrete frequency only needs the inner product of the input data and the frequency shifting



vector. Though searching the best frequency involves several loops, the computation time can be reduced by conjugate gradient method because the slope is smooth. This work can also be extended to high resolution jitter characterization of high-speed signals and eye diagram analysis.

#### ACKNOWLEDGMENT

The authors would like to thank D. Keezer and National Semiconductor for their support.

#### REFERENCES

- [1] C.E.Shannon, "Communication in the presence of noise," in *Proc. IRE*, vol. 37, Jan. 1949, pp. 10 – 21.
- [2] M. F. Duarte and Y. C. Eldar, "Structured Compressed Sensing: From Theory to Applications," in *IEEE Tran. on Signal Processing*, vol. 59, no. 9, Sep. 2011, pp. 4053 – 4085.
- [3] M. F. Duarte and R. G. Baraniuk, "Recovery of Frequency-Sparse Signals from Compressive Measurements," in *Allerton Conference on Communication, Control, and Computing*, 2010, pp. 599 – 606.
- [4] H. Choi, A. V. Gomes, and A. Chatterjee, "Signal acquisition of high-Speed periodic signals using incoherent sub-sampling and back-end signal reconstruction algorithms," in *IEEE Trans. on Very Large Scale Integration (VLSI) Systems*, vol. 19, 2011, pp. 1125 – 1135.
- [5] M. Gasior and J. L. Gonzalez, "Improving FFT frequency measurement resolution by parabolic and Gaussian spectrum interpolation," in *Proc. Beam Instrument Workshop*, vol. 732, Nov. 2004, pp. 276 – 285.
- [6] R. J. Fink, M. B. Yeary, M. Burns, and D. W. Guidry, "A DSP-Based Technique for High-Speed A/D Conversion to Generate Coherently Sampled Sequences," in *IEEE Trans. Instrum. Meas.*, vol. 52, 2003, pp. 950 – 958.
- [7] M. Burns, "Coherent undersampling digitizer for use with automatic field test equipment," May 1995.
- [8] W. V. Moer and Y. Rolain, "An improved broadband conversion scheme for the large signal network analyzer," in *IEEE Trans. Instrum. Meas.*, vol. 58, no. 2, Feb. 2009, pp. 483 – 487.
- [9] S. Haykin, *Communication Systems*. John Wiley & Sons.
- [10] A. V. Oppenheim and R. W. Schaffer, *Discrete-Time Signal Processing*. Prentice Hall.
- [11] "ADC12D1800 12-Bit, Single 3.6 GSPS Ultra High-Speed ADC," National Semiconductor, [online]. Available: <http://www.ti.com/lit/ds/symlink/adc12d1800.pdf>.